Title
Generalized Bouc-Wen model for highly asymmetric hysteresis

Permalink
https://escholarship.org/uc/item/4qk5c7vf

Journal
Journal of Engineering Mechanics-ASCE, 132(6)

ISSN
0733-9399

Authors
Song, J
Kiureghian, A D

Publication Date
2006-06-01

Peer reviewed

Generalized Bouc–Wen Model for Highly Asymmetric Hysteresis

Junho Song[1] and Armen Der Kiureghian[2]

Abstract: Bouc–Wen class models have been widely used to efficiently describe smooth hysteretic behavior in time history and random vibration analyses. This paper proposes a generalized Bouc–Wen model with sufficient flexibility in shape control to describe highly asymmetric hysteresis loops. Also introduced is a mathematical relation between the shape-control parameters and the slopes of the hysteresis loops, so that the model parameters can be identified systematically in conjunction with available parameter identification methods. For use in nonlinear random vibration analysis by the equivalent linearization method, closed-form expressions are derived for the coefficients of the equivalent linear system in terms of the second moments of the response quantities. As an example application, the proposed model is successfully fitted to the highly asymmetric hysteresis loops obtained in laboratory experiments for flexible connectors used in electrical substations. The model is then employed to investigate the effect of dynamic interaction between interconnected electrical substation equipment by nonlinear time-history and random vibration analyses.

Introduction

A memory-dependent, multivalued relation between force and deformation, i.e., hysteresis, is often observed in structural materials and elements, such as reinforced concrete, steel, base isolators, dampers, and soil profiles. Many mathematical models have been developed to efficiently describe such behavior for use in time history and random vibration analyses. One of the most popular is the Bouc–Wen class of hysteresis models, which was originally proposed by Bouc (1967) and later generalized by Wen (1976). The model has the advantage of computational simplicity, because only one auxiliary nonlinear differential equation is needed to describe the hysteretic behavior. Moreover, closed-form expressions are available for the coefficients of the equivalent linear system, which facilitate the use of the model in nonlinear random vibration analysis by the equivalent linearization method (ELM) (Wen 1980). The model is also versatile in describing various characteristics of hysteretic behavior, e.g., degrading of stiffness and strength and the pinching effect (Baber and Wen 1981; Baber and Noori 1984; Noori et al. 1986; Foliente et al. 1996), biaxial hysteresis (Park et al. 1986), and asymmetry of the peak restoring force (Wang and Wen 1998).

It has been pointed out that the Bouc–Wen class models are not in agreement with the requirements of classical plasticity theory, such as Drucker's postulate (Bažant 1978), and may produce negative energy dissipation when the unloading–reloading process occurs without load reversal (Casciati 1987; Thyagarajan and Iwan 1990). Nevertheless, the Bouc–Wen class models have been widely used in the field of structural engineering, since they greatly facilitate deterministic and stochastic dynamic analyses of real structures with reasonable accuracy. Moreover, the local violation of plasticity theory is not considered a particularly important factor in random vibration analysis, if the expected value of the restoring force is zero (Wen 1989; Hurtado and Barbat 1996).

In practice, hysteresis loops of structural elements may exhibit highly asymmetric shape due to asymmetry in geometry, boundary conditions, or material properties. For example, Fig. 1 shows the hysteresis loops of a flexible connector used in electrical substations, obtained by Filiatrault et al. (1999) in experiments with large-deformation cyclic loading. The curves of the positive displacement [Fig. 1(a)] and positive resisting force [Fig. 1(b)] are flipped onto their corresponding negative regions (dashed lines) to demonstrate the significant asymmetry in the hysteresis shape and force range. Existing Bouc–Wen class models cannot describe such highly asymmetric hysteresis unless the paramters are made functions of the response quantities. To account for the strong asymmetry of the flexible connector, Der Kiureghian et al. (2000) developed a modified Bouc–Wen model with parameters, which were complicated functions of time-varying responses. Though successful in closely fitting the experimental results, such a model is not convenient, since the dependence of the parameters on the response prohibits derivation of workable expressions for the coefficients of the equivalent linear system. Such a model is inconvenient during time-history analysis as well because it requires identifying the phase of the response and computing complicated functions at each time step.

After a careful examination of the shape-control mechanism of

[1]Assistant Professor, Dept. of Civil and Environmental Engineering, Univ. of Illinois, Urbana-Champaign, IL 61801 (corresponding author). E-mail: junho@uiuc.edu

[2]Taisei Professor of Civil Engineering, Dept. of Civil and Environmental Engineering, Univ. of California, Berkeley, CA 94720. E-mail: adk@ce.berkeley.edu
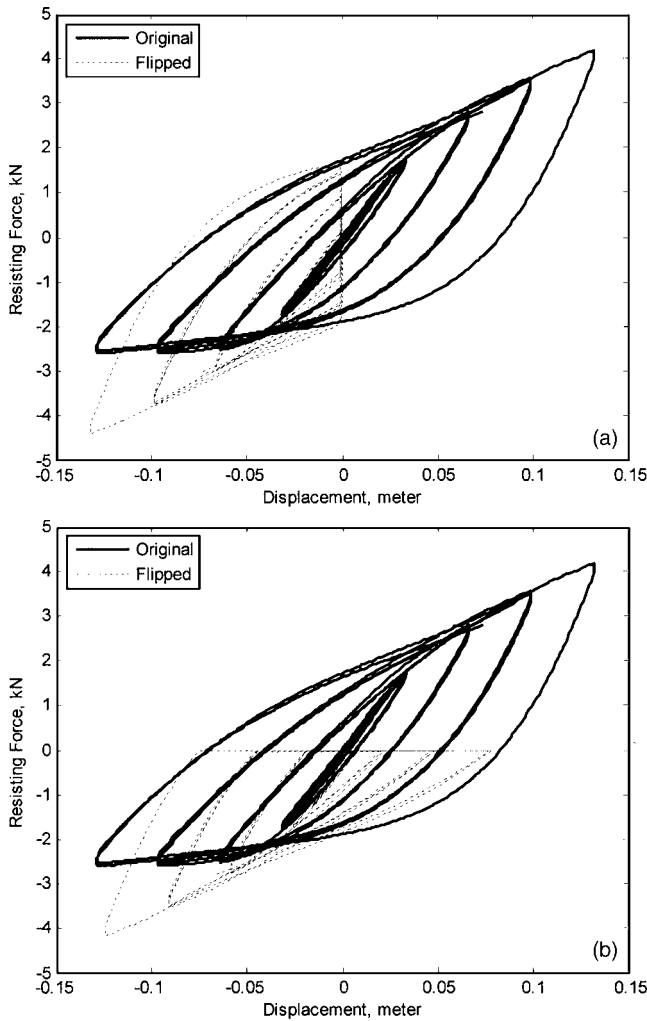
Fig. 1. Highly asymmetric hysteresis loops of flexible strap connector (PG&E 30-2021), observed by quasistatic test and comparison with curves flipped over: (a) zero-displacement; and (b) zero-force axes

existing Bouc–Wen class models, this paper introduces a generalized Bouc–Wen model that has enhanced flexibility in shape control, so that it can describe highly asymmetric hysteresis with fixed parameters. The relationship between the slopes of the hysteresis loop and the model parameters is provided for a systematic identification of the parameters based on observed data. For use in ELM, closed-form expressions are derived for the coefficients of the equivalent linear system in terms of the second moments of the response. As an example application, the proposed model is fitted to the highly asymmetric hysteretic curves of two flexible connectors used in electrical substations. The fitted model is used in nonlinear time-history and random vibration analyses of connected electrical substation equipment to investigate the effect of dynamic interaction between the equipment items under earthquake loading.

Shape-Control Mechanism of Bouc–Wen Class Models

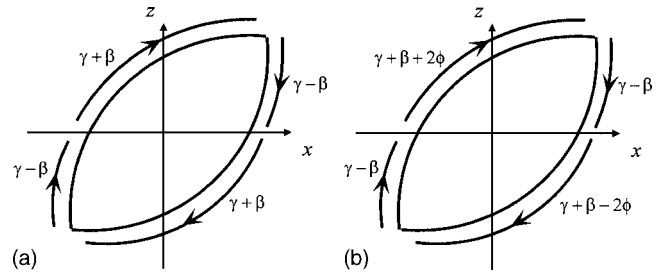For a structural element described by a Bouc–Wen class model, the resisting force is written as

Fig. 2. Values of shape-control function for: (a) original Bouc–Wen model; and (b) model by Wang and Wen

$$f_s(x,\dot{x},z) = \alpha k_0 x + (1-\alpha)k_0 z \qquad (1)$$

where x denotes the displacement; $\dot{x}=dx/dt$ denotes the velocity; $\alpha=$post- to preyield stiffness ratio; $k_0=$initial stiffness; and $z=$auxiliary variable that represents inelastic behavior. The evolution of z is determined by an auxiliary ordinary differential equation, which can be written in the form

$$\dot{z} = \dot{x}[A - |z|^n \psi(x,\dot{x},z)] \qquad (2)$$

where $\dot{z}=$derivative of z with respect to time; A and $n=$parameters that control the scale and sharpness of the hysteresis loops, respectively; and $\psi(x,\dot{x},z)=$nonlinear function of x, $\dot{x}$, and z that controls other shape features of the hysteresis loop. [Parameters for the degradation effect (Baber and Wen 1981) and an auxiliary function for the pinching effect (Baber and Noori 1984) are omitted here for simplicity. The proposed generalized Bouc–Wen model can be extended to describe such behaviors by incorporating the corresponding parameters or function.] The ψ functions of the original Bouc–Wen model (Wen 1976) and the model by Wang and Wen (1998), respectively, are

$$\psi_{\text{Bouc–Wen}} = \gamma + \beta \, \text{sgn}(\dot{x}z) \qquad (3)$$

$$\psi_{\text{Wang–Wen}} = \gamma + \beta \, \text{sgn}(\dot{x}z) + \phi[\text{sgn}(\dot{x}) + \text{sgn}(z)] \qquad (4)$$

where γ and $\beta=$parameters controlling the shape; and $\phi=$parameter that accounts for the asymmetric peak restoring force in the Wang–Wen model. Note that the displacement x does not appear in the ψ functions for these models.

Multiplying the sides of Eq. (2) by dt/dx, one obtains

$$\frac{dz}{dx} = A - |z|^n \psi(x,\dot{x},z) \qquad (5)$$

The above equation suggests that the slope of the hysteresis loop in the x-z plane, i.e., dz/dx, is controlled by the "shape-control" function $\psi(\cdot)$ within each phase determined by the signs of x, $\dot{x}$, and z.

The shape-control functions of the models in Eqs. (3) and (4) can have four different phases defined by the signs of $\dot{x}$ and z. The four phases are: (1) $(z \geq 0, \dot{x} \geq 0)$; (2) $(z \geq 0, \dot{x} < 0)$; (3) $(z < 0, \dot{x} < 0)$; and (4) $(z < 0, \dot{x} \geq 0)$. Fig. 2 shows the values of the shape-control functions for the above models within the four phases in the $x-z$ plane during a full-cycle test. The original Bouc–Wen model has only two independent values for the shape-control function: $\gamma+\beta$ for phases (1) and (3), and $\gamma-\beta$ for phases (2) and (4). The model by Wang and Wen has three independent values for the same four phases: $\gamma+\beta+2\phi$ for phase (1), $\gamma+\beta-2\phi$ for phase (3), and $\gamma-\beta$ for phases (2) and (4). Therefore, one can say that the degrees of freedom of the shape-control functions are 2 for the original Bouc–Wen model, and 3 for the
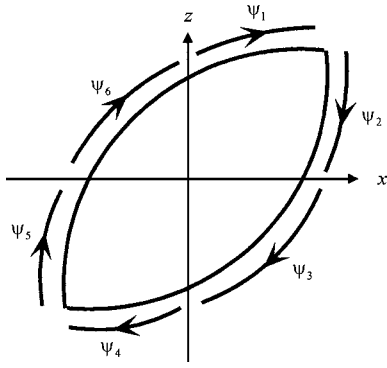
Fig. 3. Values of shape-control function for generalized Bouc–Wen model

model by Wang and Wen. The latter model can shift the hysteresis loop downward or upward by the extra degree of freedom to describe asymmetric peak forces. We make use of these findings to develop the generalized Bouc–Wen model described in the following section.

Generalized Bouc–Wen Model

As can be seen in Fig. 1, hysteresis loops are often affected not only by the signs of $\dot{x}$ and z, but also by the sign of the displacement x, because the hysteretic behavior of a structural element in tension can be different from that in compression. The existing Bouc–Wen class models do not include x in the shape-control function, and that is why they are unable to fit highly asymmetric hysteresis, unless the parameters are made functions of the response quantities, as done by Der Kiureghian et al. (2000). Therefore, it is desirable to develop a shape-control function that can assume different values for all the phases of a full cycle, as determined by the signs of x, $\dot{x}$, and z.

With this motivation, the following shape-control function is proposed:

$$\psi = \beta_1 \operatorname{sgn}(\dot{x}z) + \beta_2 \operatorname{sgn}(x\dot{x}) + \beta_3 \operatorname{sgn}(xz) + \beta_4 \operatorname{sgn}(\dot{x}) + \beta_5 \operatorname{sgn}(z)$$
$$+ \beta_6 \operatorname{sgn}(x) \quad (6)$$

where $\beta_1, \ldots, \beta_6 =$ fixed parameters. The proposed model has six degrees of freedom, as it can control the values of the shape-control function at six phases. Fig. 3 shows the six different phases of the model determined by the combinations of the signs of x, $\dot{x}$, and z during a full-cycle test. In this figure, ψ_i, $i = 1, \ldots, 6$, denotes the value of the shape-control function $\psi(x, \dot{x}, z)$ at the ith phase. Table 1 lists the sign combinations of x, $\dot{x}$, and z for the six different phases in Fig. 3 and the correspond-

Table 1. Values of the Shape-Control Function for Generalized Bouc–Wen Model

Phase	x	$\dot{x}$	z	$\psi(x,\dot{x},z)$
1	+	+	+	$\psi_1 = \beta_1 + \beta_2 + \beta_3 + \beta_4 + \beta_5 + \beta_6$
2	+	−	+	$\psi_2 = -\beta_1 - \beta_2 + \beta_3 - \beta_4 + \beta_5 + \beta_6$
3	+	−	−	$\psi_3 = \beta_1 - \beta_2 - \beta_3 - \beta_4 - \beta_5 + \beta_6$
4	−	−	−	$\psi_4 = \beta_1 + \beta_2 + \beta_3 - \beta_4 - \beta_5 - \beta_6$
5	−	+	−	$\psi_5 = -\beta_1 - \beta_2 + \beta_3 + \beta_4 - \beta_5 - \beta_6$
6	−	+	+	$\psi_6 = \beta_1 - \beta_2 - \beta_3 + \beta_4 + \beta_5 - \beta_6$

ing values of the shape-control function in terms of the parameters β_i, $i = 1, \ldots, 6$.

The linear relation between the ψ_is and β_is in Table 1 can be described in the matrix form

$$
\begin{bmatrix} \psi_1 \\ \psi_2 \\ \psi_3 \\ \psi_4 \\ \psi_5 \\ \psi_6 \end{bmatrix} =
\begin{bmatrix} 1 & 1 & 1 & 1 & 1 & 1 \\ -1 & -1 & 1 & -1 & 1 & 1 \\ 1 & -1 & -1 & -1 & -1 & 1 \\ 1 & 1 & 1 & -1 & -1 & -1 \\ -1 & -1 & 1 & 1 & -1 & -1 \\ 1 & -1 & -1 & 1 & 1 & -1 \end{bmatrix}
\begin{bmatrix} \beta_1 \\ \beta_2 \\ \beta_3 \\ \beta_4 \\ \beta_5 \\ \beta_6 \end{bmatrix} \quad (7)
$$

Since the transformation matrix in Eq. (7) is nonsingular, one can solve for β_is in terms of ψ_is by matrix inversion

$$
\begin{bmatrix} \beta_1 \\ \beta_2 \\ \beta_3 \\ \beta_4 \\ \beta_5 \\ \beta_6 \end{bmatrix} = \frac{1}{4}
\begin{bmatrix} 1 & 0 & 1 & 1 & 0 & 1 \\ 0 & -1 & -1 & 0 & -1 & -1 \\ 1 & 1 & 0 & 1 & 1 & 0 \\ 1 & -1 & 0 & -1 & 1 & 0 \\ 0 & 1 & -1 & 0 & -1 & 1 \\ 1 & 0 & 1 & -1 & 0 & -1 \end{bmatrix}
\begin{bmatrix} \psi_1 \\ \psi_2 \\ \psi_3 \\ \psi_4 \\ \psi_5 \\ \psi_6 \end{bmatrix} \quad (8)
$$

By use of the above matrix equation, the model in Eq. (6) can be fitted to experimental data in a systematic manner in conjunction with a parameter identification technique, such as the method of least squares. First, one selects a set of trial values of the ψ_is and computes the corresponding β_is by use of Eq. (8). The theoretical hysteresis loops are then plotted and compared with the experimental loops. Adjustments in the ψ_is are then made to reduce the difference between the theoretical and experimental loops by a suitable measure. For example, one can use an optimization algorithm to determine the values of ψ_is that minimize the sum of squared errors over each phase or over the entire hysteresis loop. Next, the parameters β_i are computed for the adjusted ψ_i values by use of Eq. (8). This process is continued until a set of the model parameters that minimize the difference between the theoretical and experimental hysteresis loops is achieved. Of course the search process can be conducted directly in terms of the β_i parameters without involving the intermediate parameters ψ_i. However, appropriate adjustments in the latter parameters are easier to make, particularly when fitting separately in each phase.

Equivalent Linear System

For nonlinear random vibration analysis by use of ELM, the auxiliary equation Eq. (2) with $\psi(x, \dot{x}, z)$ defined as in Eq. (6) for the generalized Bouc–Wen model is linearized in the form

$$\dot{z} + C_1 \dot{x} + C_2 x + C_3 z = 0 \quad (9)$$

where the coefficients C_1, C_2, and C_3 are determined by minimizing the expectation of the mean-square error between Eqs. (2) and (9). In case the response can be assumed to be zero-mean Gaussian, the coefficients are obtained as (Atalik and Utku 1976)

$$C_1 = E\left(\frac{\partial g}{\partial \dot{x}}\right)$$

$$C_2 = E\left(\frac{\partial g}{\partial x}\right)$$

$$C_3 = E\left(\frac{\partial g}{\partial z}\right) \qquad (10)$$

where $g = \dot{z} - \dot{x}[A - |z|^n \psi(x, \dot{x}, z)]$.

Closed-form, algebraic expressions for the coefficients in Eq. (10) are obtained by use of the following well-known relation for a zero-mean, Gaussian vector $\mathbf{y}$ and a general nonlinear function $h(\cdot)$ (Atalik and Utku 1976):

$$E[\mathbf{y}h(\mathbf{y})] = E[\mathbf{y}\mathbf{y}^T]E[\nabla h(\mathbf{y})] \qquad (11)$$

The derivation utilizes well known analytical expressions for conditional means and standard deviations of jointly normal random variables (Stone 1996). In addition, the following properties of zero-mean, Gaussian random variables X_1 and X_2 are utilized:

$$E[\text{sgn}(X_1)\text{sgn}(X_2)] = 4\int_0^\infty \int_0^\infty f_{X_1 X_2}(x_1, x_2)dx_1\,dx_2 - 1 \qquad (12)$$

$$\int_0^\infty \int_0^\infty f_{X_1 X_2}(x_1, x_2)dx_1 dx_2 = \frac{1}{4} + \frac{1}{2\pi}\sin^{-1}\rho_{X_1 X_2} \qquad (13)$$

where $f_{X_1 X_2}(x_1, x_2)$ and $\rho_{X_1 X_2}$ respectively, denote the joint probability density function and the correlation coefficient of X_1 and X_2. The latter expression is due to Sheppard (1899). For the case $n=1$, the results can be summarized in the form

$$C_1 = -A + \beta_1 E_1 + \beta_2 E_2 + \beta_3 E_3 \qquad (14)$$

$$C_2 = \beta_2 E_4 + \beta_3 E_5 \qquad (15)$$

$$C_3 = \beta_1 E_6 + \beta_2 E_7 + \beta_3 E_8 \qquad (16)$$

where the expressions for E_i, $i = 1, \ldots, 8$, in terms of the second moments of the responses are listed in Table 2. It is seen that with the Gaussian assumption, only the first three parameters β_1, β_2, and β_3, which involve the signs of the products $\dot{x}z$, $x\dot{x}$, and xz, are engaged. A different assumption regarding the distribution of the response would possibly engage all six parameters of the model. Such an analysis is currently underway.

Application to Connected Electrical Substation Equipment

As an example application, the proposed model is used to describe the hysteretic behavior of flexible strap connectors (FSCs), which are inserted for thermal expansion between electrical substation equipment items connected by a rigid bus (RB). Fig. 4 illustrates typical assemblies of an RB and two FSCs: PG&E 30-2021 and PG&E 30-2022 of Pacific Gas & Electric Company. These connectors are made of three parallel straps, each strap consisting of a pair of copper bars. See Der Kiureghian et al. (2000) for details on the dimensions and material properties of the FSCs. The generalized fitted model is used to investigate the effect of dynamic interaction between connected equipment items subjected to earthquake ground motions.

Fitting with Experimental Hysteresis Loops

Filiatrault et al. (1999) conducted quasistatic cyclic tests of the selected RB-FSCs to determine their hysteretic behavior under large-deformation cyclic loading. The resulting hysteretic curves for the two RB-FSCs considered here are shown as dashed lines

Table 2. Expressions for E_i, $i = 1, \ldots, 8$, in Eqs. (14)–(16) for Computing Coefficients of Linearized Equation for Generalized Bouc–Wen Model with $n=1$

E_i	Expression[a]
E_1	$\sqrt{\dfrac{2}{\pi}}\sigma_Z \rho_{\dot{X}Z}$
E_2	$\left(\dfrac{2}{\pi}\right)^{3/2}\sigma_Z(\rho_{XZ}\sin^{-1}\rho^*_{\dot{X}Z} + \rho_{\dot{X}Z}\sin^{-1}\rho^*_{XZ} + \sin^{-1}\rho^*_{X\dot{X}})$
E_3	$\sqrt{\dfrac{2}{\pi}}\sigma_Z\rho_{XZ}$
E_4	$\left(\dfrac{2}{\pi}\right)^{3/2}\dfrac{\sigma_{\dot{X}}\sigma_Z}{\sigma_X}\sqrt{1-\rho^2_{X\dot{X}}}\sqrt{1-\rho^2_{XZ}}\left(\sqrt{1-\rho^{*2}_{\dot{X}Z}} + \rho^*_{\dot{X}Z}\sin^{-1}\rho^*_{\dot{X}Z}\right)$
E_5	$\sqrt{\dfrac{2}{\pi}}\dfrac{\sigma_{\dot{X}}\sigma_Z}{\sigma_X}(\rho_{\dot{X}Z} - \rho_{X\dot{X}}\rho_{XZ})$
E_6	$\sqrt{\dfrac{2}{\pi}}\sigma_{\dot{X}}$
E_7	$\left(\dfrac{2}{\pi}\right)^{3/2}\sigma_{\dot{X}}(\rho_{X\dot{X}}\sin^{-1}\rho^*_{\dot{X}Z} + \sin^{-1}\rho^*_{XZ} + \rho_{\dot{X}Z}\sin^{-1}\rho^*_{X\dot{X}})$
E_8	$\sqrt{\dfrac{2}{\pi}}\sigma_{\dot{X}}\rho_{X\dot{X}}$

[a]σ denotes the standard deviation, ρ stands for the correlation coefficient, and

$$\rho^*_{\dot{X}Z} = (\rho_{\dot{X}Z} - \rho_{X\dot{X}}\rho_{XZ})/\sqrt{(1-\rho^2_{X\dot{X}})(1-\rho^2_{XZ})},$$

$$\rho^*_{XZ} = (\rho_{XZ} - \rho_{X\dot{X}}\rho_{\dot{X}Z})/\sqrt{(1-\rho^2_{X\dot{X}})(1-\rho^2_{\dot{X}Z})},$$

$$\rho^*_{X\dot{X}} = (\rho_{X\dot{X}} - \rho_{XZ}\rho_{\dot{X}Z})/\sqrt{(1-\rho^2_{XZ})(1-\rho^2_{\dot{X}Z})}.$$

in Fig. 5. The hysteretic behavior incorporates geometric nonlinearity due to the large deformation, material nonlinearity due to inelastic action, and contact and friction between the copper bars of the FSCs. The existing Bouc–Wen class models cannot represent the strong asymmetry observed in these hysteresis loops. To account for such behavior, Der Kiureghian et al. (2000) developed a modified Bouc–Wen model with parameters that are functions of time-varying responses. Fig. 5 shows the remarkably close agreement that they achieved in fitting the experimental loops. However, the fact that the parameters of this model are dependent on time renders the model inconvenient for time-history analysis and practically impossible for use in nonlinear random vibration analysis by ELM.
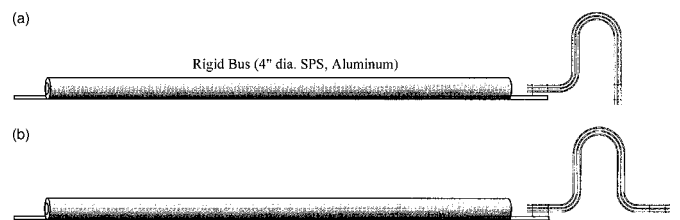

Fig. 4. Rigid bus conductors fitted with flexible strap connectors: (a) PG&E 30-2021; and (b) PG&E 30-2022
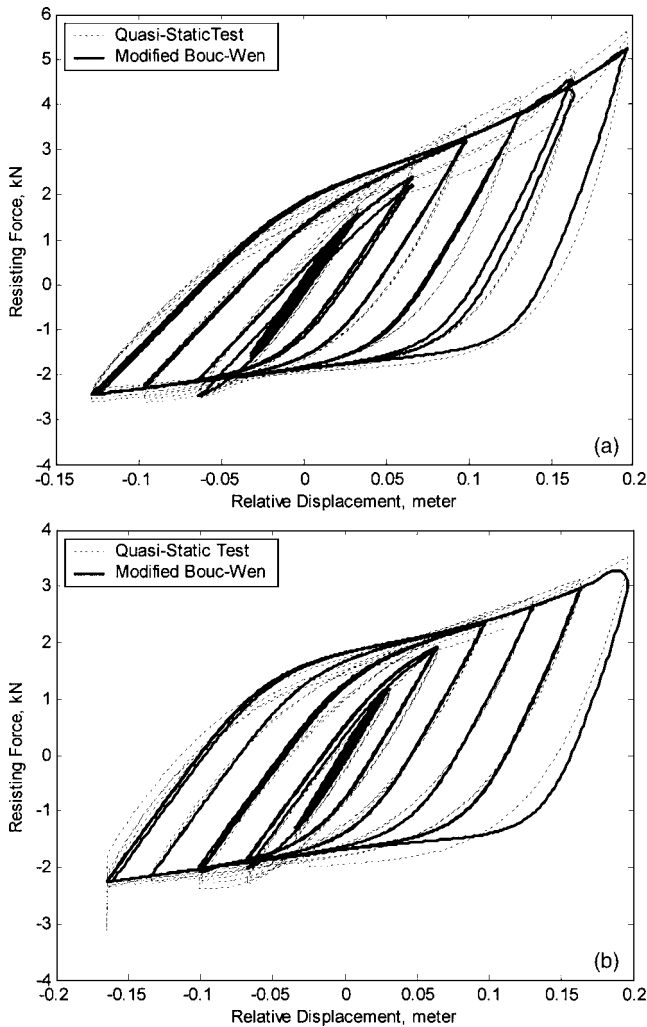
Fig. 5. Hysteretic behavior of RB-FSC as observed by Filiatrault et al. (1999) and as predicted by fitted modified Bouc–Wen model with time varying parameters: (a) PG&E 30-2021; and (b) PG&E 30-2022

Fig. 6. Hysteretic behavior of RB-FSC as observed by Filiatrault et al. (1999) and as predicted by fitted generalized Bouc–Wen model: (a) PG&E 30-2021; and (b) PG&E 30-2022

The proposed generalized Bouc–Wen model is fitted to the experimentally obtained hysteresis loops of the two FSCs, as shown in Fig. 6. The model parameters for PG&E 30-2021 are $k_0=49.2$ kN/m, $\alpha=0.1$, $A=1.0$, $n=1$, $\beta_1=0.470$, $\beta_2=-0.118$, $\beta_3=0.0294$, $\beta_4=0.115$, $\beta_5=-0.121$, and $\beta_6=-0.112$, and those for PG&E 30-2022 are $k_0=35.6$ kN/m, $\alpha=0.1$, $A=1.0$, $n=1$, $\beta_1=0.419$, $\beta_2=-0.193$, $\beta_3=0.174$, $\beta_4=0.0901$, $\beta_5=-0.156$, and $\beta_6=-0.0564$. It is evident in Fig. 6 that the model is able to represent the asymmetric hysteretic behavior of the RB-FSCs with almost as much accuracy as the model with time-varying parameters shown in Fig. 5. It is noteworthy that the good agreement of the proposed model is achieved with parameters, which remain constant throughout the loading history. This feature greatly simplifies the dynamic analysis and facilitates the use of ELM for nonlinear random vibration analysis.

Time History Analysis of Interconnected Equipment Items

When subjected to seismic excitation, interconnected equipment items may experience significant dynamic interaction, which may give rise to ampl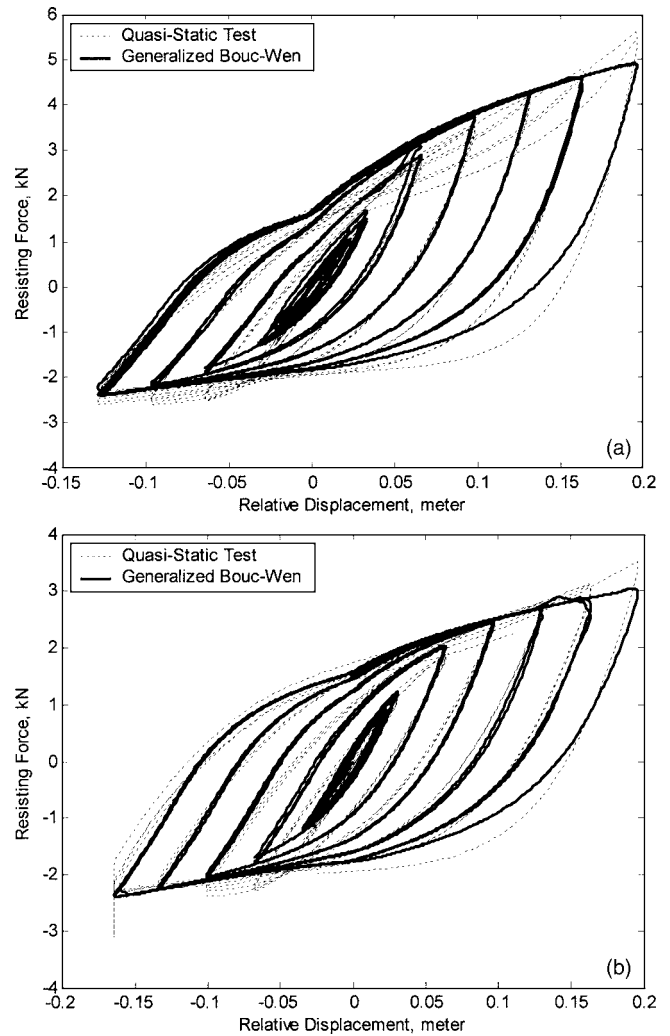ification or deamplification of the equipment responses relative to their respective stand-alone responses. Due to their flexibility and energy dissipation capacity, FSCs are known to reduce the effect of interaction. The proposed model allows us to estimate the effect of dynamic interaction in equipment items connected by FSCs having highly asymmetric hysteresis.

Consider two electrical substation equipment items connected by an RB-FSC, as illustrated in Fig. 7(a). Through the use of a displacement shape function, each equipment item is idealized as a linear single-degree-of-freedom (SDOF) oscillator, which is characterized by its effective mass m_i, effective stiffness k_i, effective damping c_i, and an effective external inertia mass l_i, for $i=1$, and 2. This idealization is depicted in Fig. 7(b), where the RB-FSC is modeled as a hysteretic element with an additional viscous damping element having the coefficient c_0. For details of the idealization and its accuracy in interaction studies, see Der Kiureghian et al. (2001) and Song (2004).

Using the SDOF model for each equipment item, the equation of motion of the connected system in Fig. 7(b) is described in a matrix form as

$$\mathbf{M\ddot{u}} + \mathbf{C\dot{u}} + \mathbf{R}(\mathbf{u}, \dot{\mathbf{u}}, z) = -\mathbf{L}\ddot{x}_g \qquad (17)$$
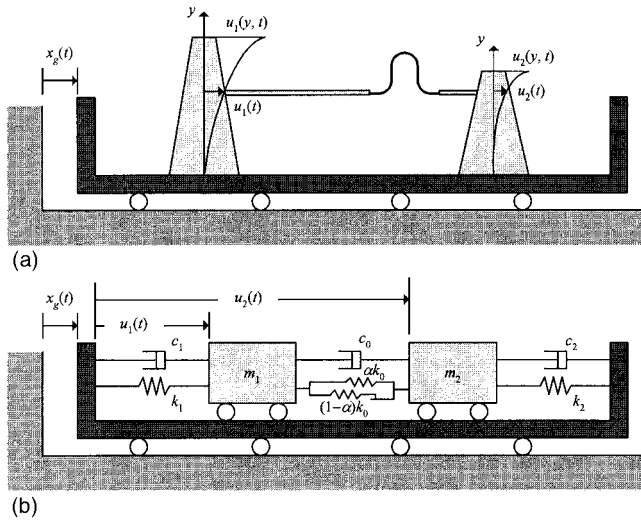
where

Fig. 7. Mechanical models of equipment items connected by RB-FSC: (a) RB-FSC-connected system; and (b) idealized system with SDOF equipment models
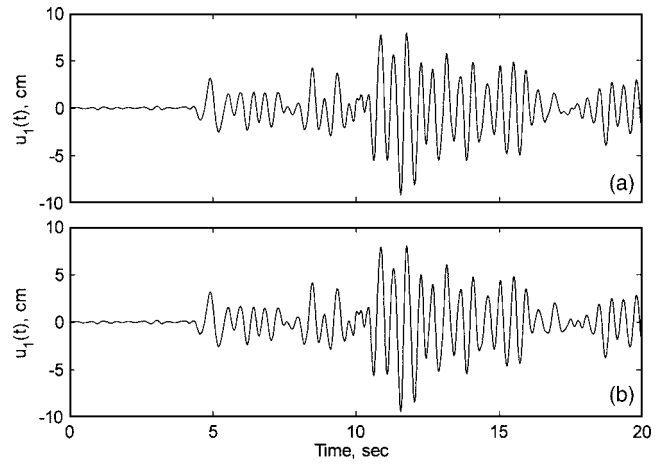

Fig. 8. Displacement time histories of lower-frequency equipment item in RB-FSC (PG&E 30-2022) connected system for Tabas LN record: (a) modified Bouc–Wen model with time-varying parameters; and (b) generalized Bouc–Wen model

$$\mathbf{u} = \begin{Bmatrix} u_1(t) \\ u_2(t) \end{Bmatrix}$$

$$\mathbf{M} = \begin{bmatrix} m_1 & 0 \\ 0 & m_2 \end{bmatrix}$$

$$\mathbf{C} = \begin{bmatrix} c_1 + c_0 & -c_0 \\ -c_0 & c_2 + c_0 \end{bmatrix} \tag{18}$$

$$\mathbf{R}(\mathbf{u},\dot{\mathbf{u}},z) = \begin{Bmatrix} k_1 u_1(t) - f_s[\Delta u(t), \Delta \dot{u}(t), z(t)] \\ k_2 u_2(t) + f_s[\Delta u(t), \Delta \dot{u}(t), z(t)] \end{Bmatrix}$$

$$\mathbf{L} = \begin{Bmatrix} l_1 \\ l_2 \end{Bmatrix} \tag{19}$$

where $\ddot{x}_g$=base acceleration; $u_i(t)$=displacement of the ith equipment item at its attachment point relative to the base; $\Delta u(t) = u_2(t) - u_1(t)$=relative displacement between the two equipment items; and the function $f_s(\Delta u, \Delta \dot{u}, z)$ denotes the resisting force of the RB-FSC as described by Eq. (1) with Δu and $\Delta \dot{u}$ replacing x and $\dot{x}$, respectively. The auxiliary variable z is defined by the generalized Bouc–Wen model as described by Eqs. (2) and (6).

Among several methods available for solving the above system of nonlinear differential equations, one convenient method is to reduce the second-order differential equation to the first order and then solve it by use of a numerical algorithm. The equations of motion of the connected system in Eqs. (17)–(19) are reduced to a first-order, state-space equation of the form

$$\dot{\mathbf{y}} = \mathbf{g}(\mathbf{y}) + \mathbf{f} \tag{20}$$

where

$$\mathbf{y} = \{u_1 \ \dot{u}_1 \ u_2 \ \dot{u}_2 \ z\}^{\mathrm{T}} \tag{21}$$

$$\mathbf{g}(\mathbf{y}) = \begin{Bmatrix} \dot{u}_1 \\ -\left(\dfrac{k_1 + \alpha k_0}{m_1}\right)u_1 - \left(\dfrac{c_1 + c_0}{m_1}\right)\dot{u}_1 + \dfrac{\alpha k_0}{m_1}u_2 + \dfrac{c_0}{m_1}\dot{u}_2 + \dfrac{(1-\alpha)k_0}{m_1}z \\ \dot{u}_2 \\ \dfrac{\alpha k_0}{m_2}u_1 + \dfrac{c_0}{m_2}\dot{u}_1 - \left(\dfrac{k_2 + \alpha k_0}{m_2}\right)u_2 - \left(\dfrac{c_2 + c_0}{m_2}\right)\dot{u}_2 - \dfrac{(1-\alpha)k_0}{m_2}z \\ \dot{z}(\Delta u, \Delta \dot{u}, z) \end{Bmatrix} \tag{22}$$

$$\mathbf{f} = \left\{ 0 \ -\dfrac{l_1}{m_1}\ddot{x}_g \ 0 \ -\dfrac{l_2}{m_2}\ddot{x}_g \ 0 \right\}^{\mathrm{T}} \tag{23}$$

The fourth-order, adaptive Runge–Kutta–Fehlberg algorithm (Fehlberg 1969) is used with a relative tolerance of 10^{-6} to solve the above system of equations for a deterministically specified base acceleration.

As an example, we consider a system having the parameter values m_1=1,090 kg, m_2=545 kg, k_1=172 kN/m, k_2=538 kN/m, $l_1/m_1 = l_2/m_2 = 1.0$, and $\zeta_i = c_i/(2\sqrt{m_i k_i}) = 0.02$, $i = 1, 2$. Note that equipment 1 has the stand-alone natural frequency $\sqrt{172,000/1,090}/2\pi = 2$ Hz, while the stand-alone natural frequency of equipment 2 is $\sqrt{538,000/545}/2\pi = 5$ Hz. For the RB-FSC, PG&E 30-2022 is selected with the hysteretic model parameter values given in the previous subsection. No viscous damping is assumed for the RB-FSC so that c_0=0. The connected system is assumed to be subjected to the longitudinal record of the Tabas 1978 earthquake (Tabas LN). Hereafter, we refer to equipment 1 as the lower-frequency equipment item, and equipment 2 as the higher-frequency equipment item.

Figs. 8 and 9 show the displacement time histories of the lower- and higher-frequency equipment items, respectively, as computed using the generalized Bouc–Wen model and the model developed by Der Kiureghian et al. (2000) with time-varying parameters. Recall that the latter model practically coincides with the experimental hysteresis loops. Hence, the responses computed by this model can be considered as the "exact" behavior. By comparing the pair of results in each figure, it is seen that the responses computed using the proposed generalized Bouc–Wen model are practically identical to the "exact" results. In particular, the maximum relative displacement between the two equipment
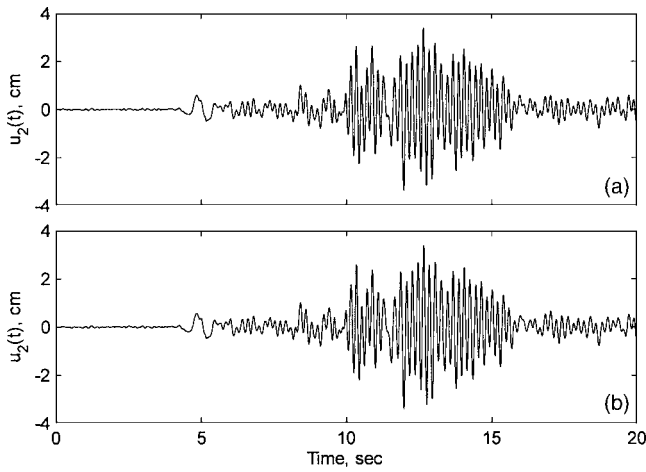
Fig. 9. Displacement time histories of higher-frequency equipment item in RB-FSC (PG&E 30-2022)-connected system for Tabas LN record: (a) modified Bouc–Wen model with time-varying parameters; and (b) generalized Bouc–Wen model

items predicted by both models is 0.098 m, which shows that the RB-FSC experiences significant nonlinear deformation. This is confirmed by the hysteresis loops depicted in Fig. 10 for both models. It is noted that the time-history analysis with the generalized Bouc–Wen model is much more efficient, since its parameters are not functions of time.

Nonlinear Random Vibration Analysis of Interconnected Equipment Items

Due to the highly uncertain nature of earthquake ground motions, for design purposes it is important to have an estimate of the response based on a stochastic model of the ground motion rather than any selected accelerogram. Moreover, as we have seen, the behavior of an RB-FSC in general is nonlinear and hysteretic in nature. These two factors give rise to the need for a nonlinear random vibration analysis method.
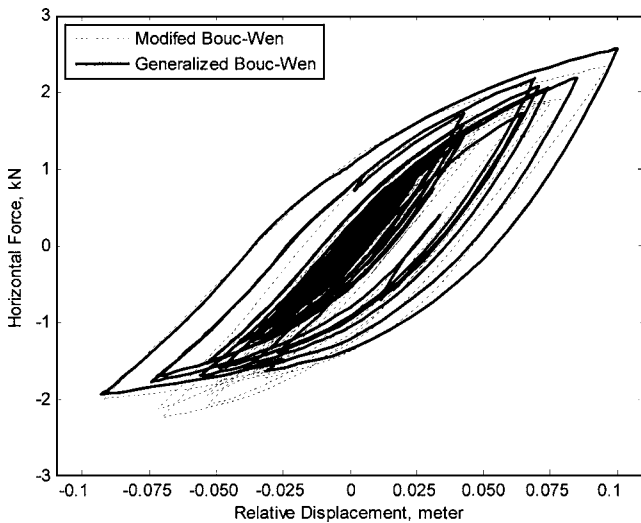

Fig. 10. Force-elongation hysteresis loops of RB-FSC (PG&E 30-2022) in interconnected system subjected to Tabas LN record

In the field of earthquake engineering, the Bouc–Wen class hysteresis models have been widely used for nonlinear random vibration analysis by use of the ELM (Wen 1980; Baber and Wen 1981; Wen and Yeh 1989; Schuëller et al. 1994; Kimura et al. 1994; Hurtado and Barbat 1996). Closed-form expressions available for the coefficients of the corresponding equivalent linear systems greatly facilitate the iterative processes of ELM for these models. Herein, the proposed generalized Bouc–Wen model is applied to ELM analysis of the interconnected equipment system to investigate the effect of dynamic interaction.

Assuming the response is nearly Gaussian, the nonlinear differential equation in the last row of Eq. (22) is replaced by the equivalent linear equation Eq. (9). As a result, the nonlinear state-space equation Eq. (20) is linearized into $\dot{\mathbf{y}}=\mathbf{G}\mathbf{y}+\mathbf{f}$, where $\mathbf{G}$ denotes the equivalent linear coefficient matrix. When the base acceleration $\ddot{x}_g$ is a stationary, delta-correlated process (including white noise), the differential equation governing the covariance matrix $\mathbf{S}=E[\mathbf{y}\mathbf{y}^T]$ of the state vector $\mathbf{y}$ must satisfy (Lin 1967)

$$\mathbf{G}\mathbf{S}^T + \mathbf{S}\mathbf{G}^T + \mathbf{B} = \mathbf{0} \tag{24}$$

where $B_{ij}=0$ except $B_{22}=2\pi(l_1/m_1)^2\Phi_0$ and $B_{44}=2\pi(l_2/m_2)^2\Phi_0$, where $\Phi_0=$power spectral density of $\ddot{x}_g$. This equation is solved by an iterative scheme (Wen 1980), since matrix $\mathbf{G}$ involves the coefficients of the equivalent linear system, which are functions of the second moments in the covariance matrix $\mathbf{S}$. An equation of the form Eq. (24) can also be derived for the case of a filtered white-noise input process $\ddot{x}_g(t)$ by augmenting the equations of motion with the equation of the filter (Wen 1980; Song 2004). Here, we consider the filter suggested by Clough and Penzien (1993), which characterizes the ground acceleration process with a Kanai—Tajimi power spectral density having a dominant frequency of ω_g (the filter frequency), bandwidth parameter ζ_g (the filter damping ratio), and an intensity parameter Φ_0.

In order to quantify the effect of dynamic interaction in random vibration analysis, Der Kiureghian et al. (1999) introduced the ratio of root-mean-square (rms) responses

$$R_i = \frac{\text{rms}[u_i(t)]}{\text{rms}[u_{i0}(t)]} \quad i=1,2 \tag{25}$$

where rms[·] denotes a rms value, and $u_i(t)$ and $u_{i0}(t)$ respectively, denote the displacements of equipment i in the connected and stand-alone configurations at time t. For a stationary response, these ratios are of course invariant of time. It should be clear that a response ratio with a value greater (respectively, smaller) than unity indicates that the interaction effect amplifies (respectively, deamplifies) the response of the equipment item in the connected system relative to the response in its stand-alone configuration. Thus, R_is are good measures of the dynamic interaction effect between the connected equipment items.

As an example, consider two equipment items connected by three RB-FSCs. The system parameters have the values $m_1=401$ kg, $m_2=200$ kg, $k_1=15.8$ kN/m, $k_2=198$ kN/m, $l_1/m_1=l_2/m_2=1.0$, $c_0=0$, and $\zeta_i=c_i/(2\sqrt{m_ik_i})=0.02$, $i=1,2$. The selected FSC is PG&E 30-2022, which is idealized by the generalized Bouc–Wen model with the parameter values describe earlier. Since three RB-FSCs are used, the initial stiffness is $k_0=3\times35.6=106.8$ kN/m. For the ground acceleration, a zero-mean, stationary Gaussian, filtered white-noise process having the Kanai–Tajimi power spectral density with $\omega_g=5\pi$ rad/s and $\zeta_g=0.6$ is used. The intensity parameter, Φ_0, is varied to examine the variation in the nonlinearity of the system with increasing intensity of the ground motion, as measured in terms of the rms
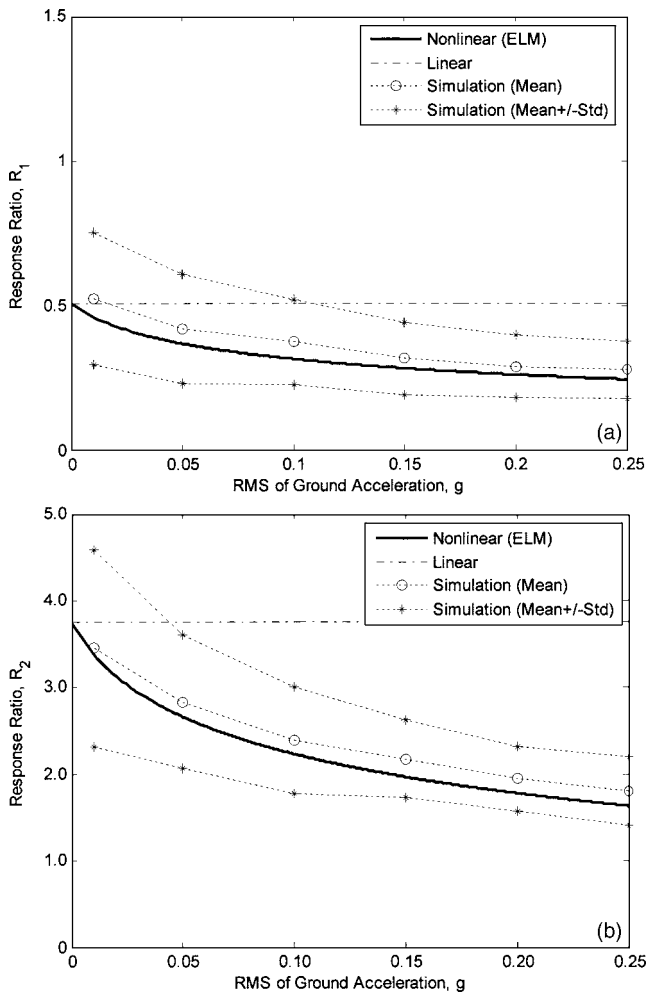
Fig. 11. Response ratios for equipment items connected by three parallel RB-FSC (PG&E 30-2022): (a) lower-frequency equipment item; and (b) higher-frequency equipment item

acceleration in units of gravity acceleration. Roughly speaking, the rms acceleration is a factor $1/2$ to $1/3$ of the peak ground acceleration.

The rms response ratios in Eq. (25) are evaluated by three different approaches: (1) nonlinear random vibration analysis by use of the ELM for the system with the proposed generalized Bouc–Wen model of the FSC; (2) linear random vibration analysis by use of the initial stiffness of the RB-FSC obtained by setting $\alpha = 1.0$ in the nonlinear random vibration analysis; and (3) nonlinear time-history analyses by use of 100 simulated ground motions based on the specified power spectral density. In the latter case, assuming ergodicity of the response process, the rms values are computed by time averaging the response samples over a sufficiently long interval of time.

Fig. 11(a) shows a plot of the response ratio of the lower-frequency equipment item, R_1, versus the rms value of the ground acceleration. Fig. 11(b) shows a similar plot for the response ratio R_2 of the higher-frequency equipment item. It is seen that the estimate based on the linear random vibration analysis is a constant response ratio, independent of the intensity of the ground motion. This is because the responses of the linear systems representing the stand-alone and connected configurations are amplified by the same ratio when the seismic intensity is increased. As observed earlier by Der Kiureghian et al. (1999), the interaction

between the two connected equipment items results in deamplification of the response of the lower-frequency equipment and amplification of the response of the higher-frequency equipment relative to their respective stand-alone responses. For the linear system, the de-amplification in the lower-frequency item is a factor of 0.5, whereas the amplification in the higher-frequency equipment item is a factor of 3.7. The estimates by ELM show a significant reduction in the response ratios of both equipment items, depending on the intensity of the ground motion. Two factors contribute to this reduction: (1) energy dissipation by the RB-FSC, which tends to reduce all responses of the connected system relative to those of the linear system; and (2) softening of the RB-FSC, which tends to reduce the interaction effect between the two connected equipment items. The reduction in the interaction effect tends to increase the response ratio for the lower-frequency equipment item and reduce the response ratio of the higher-frequency equipment item. The overall result is a reduction in the response ratios of both equipment items with increasing intensity of the ground motion.

To examine the accuracy of the response predictions by the ELM, time-history analyses are carried out for 100 sample functions of the ground motion, which are simulated in accordance with the specified power spectral density. As mentioned earlier, the rms value for each response sample is computed by time averaging over a 10 s period of stationary response. The sample of 100 rms estimates are then used to compute the mean and standard deviation of the response ratio according to Eq. (25). The mean and mean ±1 SD of the estimated response ratios are shown in Fig. 11. The results show reductions in the response ratios with increasing intensity of the ground motion, in close agreement with the ELM predictions.

It is also worthwhile to note in Fig. 11 that the time-history results show significant dispersion, even though the 100 sample ground motions are consistent with a single power spectral density. This indicates the high sensitivity of the interaction effect and the response ratios on the details of the ground motion. Under these conditions, clearly a stochastic analysis method is essential. In spite of its approximate nature, the ELM, incorporating the proposed generalized Bouc–Wen model, offers a viable and accurate alternative for this purpose.

Summary and Conclusions

A generalized Bouc–Wen model is developed to describe highly asymmetric hysteresis with applicability to nonlinear time-history analysis and nonlinear random vibration analysis by use of the ELM. Based on an anatomic examination of the shape-control mechanism of existing Bouc–Wen class models, a new Bouc–Wen-type model is proposed that offers enhanced flexibility in shape control so that it can describe highly asymmetric hysteresis loops with time-invariant parameters. This is made possible by introducing an equation that describes the relation between the shape-control parameters and the slopes of the hysteresis loop in different phases. The equation helps to efficiently identify the shape-control parameters in conjunction with available parameter identification methods.

For nonlinear random vibration analysis by use of the ELM, closed-form expressions for the coefficients of the equivalent linear system are derived in terms of the second moments of the responses for the case of zero-mean, stationary Gaussian processes. As an example application, the proposed model is used to describe the hysteretic behavior of FSCs, which are commonly

employed in the industry to connect electrical substation equipment items. The proposed model successfully describes the asymmetric hysteresis loops of the existing FSCs as observed in laboratory experiments.

The proposed model is used to investigate the effect of dynamic interaction between connected equipment items. Nonlinear time-history and ELM random vibration analyses consistently show that the interaction effect tends to deamplify the response of the lower-frequency equipment relative to its stand-alone response, and to amplify the response of the higher-frequency item relative to its stand-alone response. With increasing intensity of the ground motion, the interaction effect decreases due to increasing flexibility of the connecting FSC as it yields.

Acknowledgments

References

Atalik, T. S., and Utku, S. (1976). "Stochastic linearization of multi-degree-of-freedom nonlinear systems." *Earthquake Eng. Struct. Dyn.*, 4, 411–420.

Baber, T. T., and Noori, M. N. (1984). "Random vibration of pinching hysteretic systems." *J. Eng. Mech.*, 110(7), 1036–1049.

Baber, T. T., and Wen, Y. K. (1981). "Random vibration hysteretic, degrading systems." *J. Eng. Mech. Div., Am. Soc. Civ. Eng.*, 107(6), 1069–1087.

Bažant, Z. (1978). "Endochronic inelasticity and incremental plasticity." *Int. J. Solids Struct.*, 14, 691–714.

Bouc, R. (1967). "Forced vibration of mechanical system with hysteresis (Abstract)." *Proc., 4th Conf. on Nonlinear Oscillation*, Prague, Czechoslovakia.

Casciati, F. (1987). "Nonlinear stochastic dynamics of large structural systems by equivalent linearization." *Proc., 5th Int. Conf. on Application of Statistics and Probability in Soil and Structural Engineering*, ICASP5, Vancouver, B.C., Canada.

Clough, R., and Penzien, J. (1993). *Dynamics of structures*, McGraw-Hill, New York.

Der Kiureghian, A., Hong, K.-J., and Sackman, J. L. (2000). "Further studies on seismic interaction in interconnected electrical substation equipment." *PEER Rep. No. 2000/01*, Univ. of California, Berkeley, Calif.

Der Kiureghian, A., Sackman, J. L., and Hong, K.-J. (1999). "Interaction in interconnected electrical substation equipment subjected to earthquake ground motions." *PEER Rep. No. 1999/01*, Univ. of California, Berkeley, Calif.

Der Kiureghian, A., Sackman, J. L., and Hong, K.-J. (2001). "Seismic interaction in linearly connected electrical substation equipment." *Earthquake Eng. Struct. Dyn.*, 30, 327–347.

Fehlberg, E. (1969). "Klassische Runge-Kutta formeln fünfter und siebenter ordnung mit schrittweitenkontrolle." *Computing*, 4, 93–106.

Filiatrault, A., Kremmidas, S., Elgamal, A., and Seible, F. (1999). "Substation equipment interaction—Rigid and flexible conductor studies." *Rep. No. SSRP-99/09*, Univ. of California, San Diego, Calif.

Foliente, G. C., Singh, M. P., and Noori, M. N. (1996). "Equivalent linearization of generally pinching hysteretic, degrading systems." *Earthquake Eng. Struct. Dyn.*, 25, 611–629.

Hurtado, J. E., and Barbat, A. H. (1996). "Improved stochastic linearization method using mixed distributions." *Struct. Safety*, 18(1), 49–62.

Kimura, K., Yasumuro, H., and Sakata, M. (1994). "Non-Gaussian equivalent linearization for stationary random vibration of hysteretic system." *Probab. Eng. Mech.*, 9, 15–22.

Lin, Y. K. (1967). *Probabilistic theory of structural dynamics*, McGraw–Hill, New York.

Noori, M. N., Choi, J., and Davoodi, H. (1986). "Zero and nonzero mean random vibration analysis of a new general hysteresis model." *Probab. Eng. Mech.*, 1(4), 192–201.

Park, Y. J., Wen, Y. K., and Ang, A. H. S. (1986). "Random vibration of hysteretic systems under bi-directional ground motion." *Earthquake Eng. Struct. Dyn.*, 14, 543–547.

Schuëller, G. I., Pandey, M. D., and Pradlwarter, H. J. (1994). "Equivalent linearization (EQL) in engineering practice for aseismic design." *Probab. Eng. Mech.*, 9, 95–102.

Sheppard, W. F. (1899). "On the application of the theory of the error to cases of normal distribution and normal correlation." *Philos. Trans. R. Soc. London, Ser. A*, 192, 101–167.

Song, J. (2004). "Seismic response and reliability of electrical substation equipment and system." Ph.D. thesis, Univ. of California, Berkeley, Calif.

Stone, C. J. (1996). *A course in probability and statistics*, Duxbury, Belmont, Calif.

Thyagarajan, R. S., and Iwan, W. D. (1990). "Performance characteristics of a widely used hysteretic model in structural dynamics." *Proc., 4th U.S. National Conf. Earthquake Engineering*, Palm Springs, Calif.

Wang, C.-H., and Wen, Y. K. (1998). "Reliability and redundancy of pre-northridge low-rise steel building under seismic excitation." *Rep. No. UILU-ENG-99-2002*, Univ. Illinois at Urbana-Champaign, Champaign, Ill.

Wen, Y. K. (1976). "Method for random vibration of hysteretic systems." *J. Eng. Mech. Div., Am. Soc. Civ. Eng.*, 102(2), 249–263.

Wen, Y. K. (1980). "Equivalent linearization for hysteretic systems under random excitation." *Trans. ASME*, 47, 150–154.

Wen, Y. K. (1989). "Methods of random vibration for inelastic structures." *Appl. Mech. Rev.*, 42(2), 39–52.

Wen, Y. K., and Yeh, C. H. (1989). "Biaxial and torsional response of inelastic structures under random excitation." *Struct. Safety*, 6, 137–152.